NMRlipids IV: Headgroup & glycerol backbone structures, and cation binding in bilayers with PS lipids

O. H. Samuli Ollila[1, 2, *]

[1] *Institute of Organic Chemistry and Biochemistry, Academy of Sciences of the Czech Republic, Prague 6, Czech Republic*
[2] *Institute of Biotechnology, University of Helsinki*

(Dated: December 21, 2017)

Primarily measured but also simulated NMR order parameters will be collected also for other than phophatidylcholine (these are discussed in NMRlipids I) headgroup. The information will be used to understand structural differences between different lipid molecules in bilayers.

INTRODUCTION

In NMRlipids I and II project we were looking for a MD model which would correctly reproduce headgroup and glycerol backbone structures and cation binding for PC lipid bilayers [1, 2]. Here we extend the same goal for lipids with negatively charged PS headgroup. Chemical structure of PS headgroup together with other common biological lipids is shown in Fig. 1.

Absolute values of experimental order parameters for different lipid headgroups are collected from the literature in Fig. 2. Since order parameter signs are known only for PC, only absolute values are shown. Main conclusions regarding the structure of different common lipid headgroups in the literature are

1) glycerol backbone structures are largely similar irrespectively of the headroup [3],
2) glycerol backbone and headgroup structure and behaviour are similar in model membranes and in bacteria [3–5],
3) headgroup structures are similar in PC, PE and PG lipids, while headgroup is more rigid in PS lipids [6, 7].

Careful discussion and analysis of structural details of PE, PG or PS headgroups is not available, in contrast to PC lipids (see [1] and references therein).

As shown in Fig. 3, order parameters of PC headgroup behave in various lipid mixtures as expected from the electrometer concept [4, 12], i.e., order parameters increase when anionic lipids are mixed with PC and decrease with cationic surfactants. The changes with the addition of neutral lipids is significantly smaller.

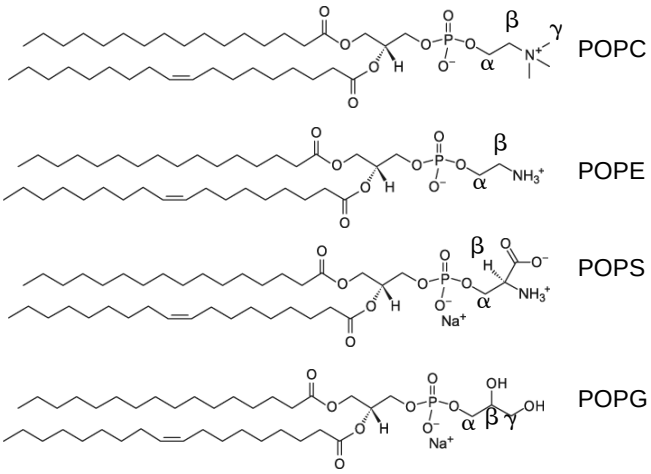

FIG. 1: Chemical structures and labels for the headgroup carbons.

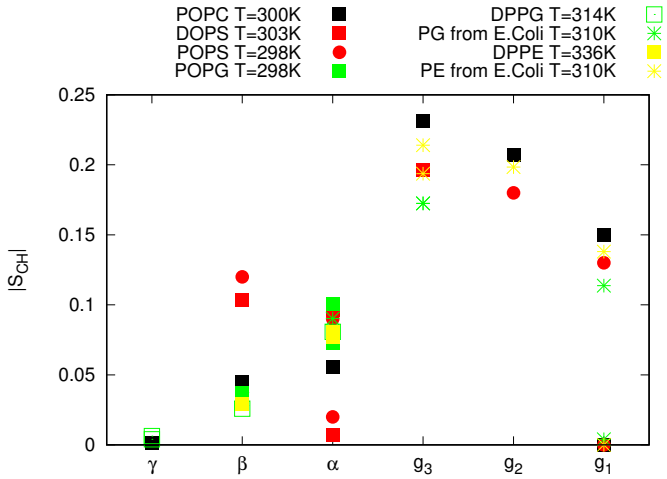

FIG. 2: Absolute values of order parameters for headgroup and glycerol backbone with different headgroups from experiments. POPC values are from [8], DOPS from [9] contains 0.1M of NaCl, POPG from [10] contains 10nM PIPES, DPPG from [6] contains 10mM PIPES and 100mM NaCl, DPPE from [11], E.coliPE and E.coliPG are from [3].

RESULTS AND DISCUSSION

Headgroup and glycerol backbone structure in simulations and experiments of PS lipid bilayers

The headgroup order parameters of DOPS and POPS bilayers from different experiments and simulations are shown in Figs. 4. None of the tested models gives satisfactory agreement with experiments for order parameters in headgroup α and β carbons.

Glycerol backbone order parameters seems similar in all models, except in Slipids. Slipid model do not correctly capture the glycerol backbone structure, as already observed previously for PC lipids [1]. The glycerol backbone structures

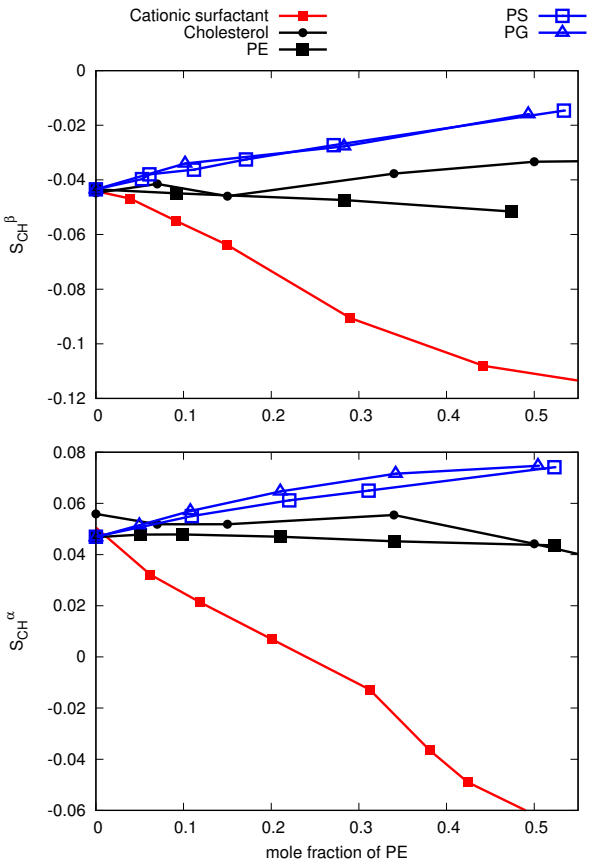

FIG. 3: PC headgroup order parameters from experiments of mixtures with PE, PS, PG and cholesterol [4, 8, 13]. Signs are determined as discussed in [1, 14].

between PC and PS lipids simulated with Slipids are compared with the structures simulated with CHARMM36 in Fig. 6. The differences in sampled conformation leading to the order parameter differences are clearly visible in the figure.

2.Dihedral angle distribtions in Fig. 14 should be included in the discussion.

Headgroup structure in PS and PC mixtures

The headgroup order parameters of POPC mixed with PS lipids are shown in Fig. 7 from different simulation model and experiments [4] with different mole fractions. As already discussed previosly, the PC lipid headgroup behaviour follows the electrometer concept in experiments when mixed with other lipids, i.e., the order parameters increase when mixed with negatively charged lipids (PS, PI, CL, PA and PG) remains almost unchaged when mixed with neutral lipids (PE and SM) [4]. This is not the case in simulation data shown in Fig. 7.

5.More data to be collected before discussion.

The headgroup order parameters of PS mixed with varying amounts of PC from simulations and experiments [10, 15] are shown in Fig. **??**. The effect of increasing amount of PC to PS

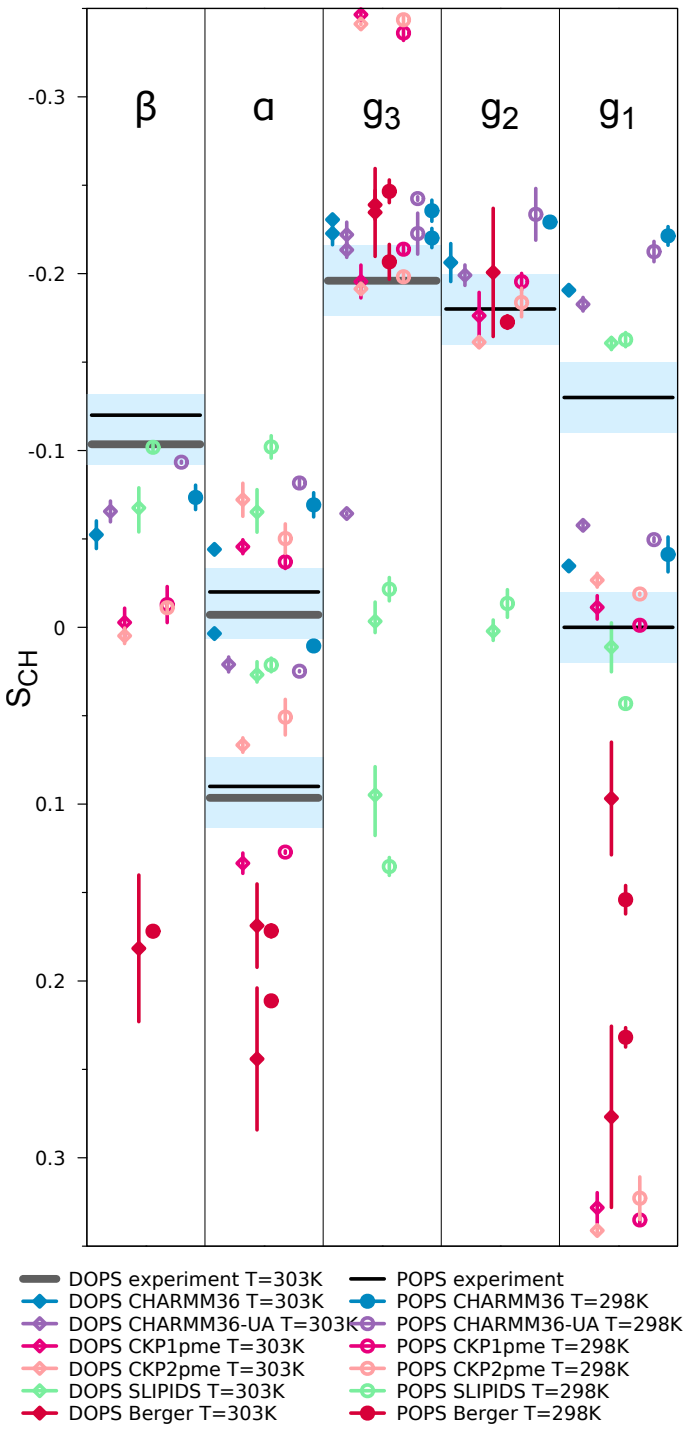

FIG. 4: Order parameters for PS headgroup and glycerol backbone from simulations with different models and experiments without $CaCl_2$ Experimental data from [9] contains 0.1M of NaCl. Signs are taken from experiments for POPS described in Supplementary Information. The vertical bars shown for the computational values are not error bars, but demonstrate that for these systems we had at least two data sets; the ends of the bars mark the extreme values from the sets, and the dot marks their measurement-time-weighted average.

1.Check and report all the counterions.

	β	α	g_3	g_2	g_1	Σ
CHARMM 36	M	M F	M	M	**M** F	8
CHARMM 36-UA	M	M	M	M	**M** F	8
GROMOS-CKP1	**M**	M **F**	**M F**		**M F**	14
GROMOS-CKP2	**M**	M F	**M F**		**M F**	14
Slipid	M	**M**	**M F**	**M**	M **F**	14
Berger	**M**	**M F**	M F	M	**M** F	15

FIG. 5: Rough subjective ranking of force fields based on Figure 4. Here M indicates a magnitude problem, F a forking problem; letter size increases with problem severity. Color scheme: within experimental error (dark green), almost within experimental error (light green), clear deviation from experiments (light red), and major deviation from experiments (dark red). The Σ-column shows the total deviation of the force field, when individual carbons are given weights of 0 (matches experiment), 1, 2, and 4 (major deviation). For full details of the assessment, see Supplementary Information.

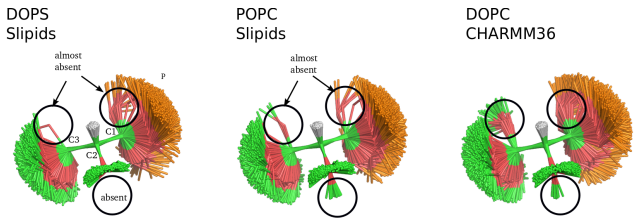

FIG. 6: Snapshots overlayed from different simulations for glycerol backbone region by Pavel Buslaev.

headgroup seems to qualitatively incorrect in CHARMM36 simulations. The β-carbon order parameter increases in experiment, but decreases in simulations with both tested counterions (Na+ and K+). Larger α-carbon order parameter decreases with the addition of PC in experiment, while the lower remains unchanged. In simulations the larger increases and the lower decreases. Interestingly, the α-carbon order parameters are closer to experiments in pure PS system with K+ counterions than with Na+.

Ca^{2+} binding affinity in bilayers with negatively charged PS lipids

PC lipid headgroup order parameters can used to measure ion binding affinity, because their magnitude is proportional to the amount of bound charge in bilayer [2, 12]. The molecular electrometer concept can be used also for bilayers containing PC lipids mixed with charged lipids [10, 15, 16]. This is demonstrated in Fig. 8, showing the changes of PC headgroup order parameters as a function of $CaCl_2$ concentration in the presence of different amounts of negatively charged PS or PG lipids. The decrease of order parameters with $CaCl_2$ is more pronounced for systems with more negatively charged lipids.Order parameters reach the values of pure PC bilayer close to $CaCl_2$ concentrations of $\sim$ 50-300mM. At this point the Ca2+ binding presumably fully cancels the charge from negative lipids and overcharging occurs above these concenterations. The interpretation of this data and some other results has been that [5]

> *"(i) Ca^{2+} binds to neutral lipids (phosphatidylcholine, phosphatidylethanolamine) and negatively charged lipids (phosphatidylglycerol) with approximately the same binding constant of K = 10-20 M^{-1};*
> *(ii) the free Ca^{2+} concentration at the membrane interface is distinctly enhanced if the membrane carries a negative surface charge, either due to protein or to lipid;*
> *(iii) increased inter-facial Ca^{2+} also means increased amounts of bound Ca^{2+} at neutral and charged lipids;*
> *(iv) the actual binding step can be described by a Langmuir adsorption isotherm with a 1 lipid:1 Ca^{2+} stoichiometry, provided the interfacial concentration C_M, is used to describe the chemical binding equilibrium."*

Before using headgroup order parameters to compare ion binding affinity between simulations and experiments, the response of the order parameters to bound charge has to be quantified. The response of headgroup order parameters to the fixed amount of cationic surfactants in POPC bilayer is compared between simulations and experiments [13] In Fig. 9. The figure shows that the order parameters are too sensitive to bound charge in Lipid14 model, while CHARMM36 is in better agreement with experiments. This has to be taken into account when analysin the binding affinities.

6.When we have more data for Ca binding to PS containing bilayers, the discussion will be updated and PG results moved to other manuscript. Comparison of Ca2+ binding in PG between CHARMM36 simulations and experiments [10] is shown in Fig. 10. The decrease of α order parameter is in agreement with experiments, while decerase of β order parameter is overestimated. The result is very similar to the results with PC in NMRlipids II publication [2]. It should be, however, noted that the β-order parameters are not actually measured for PG, but they are cal-

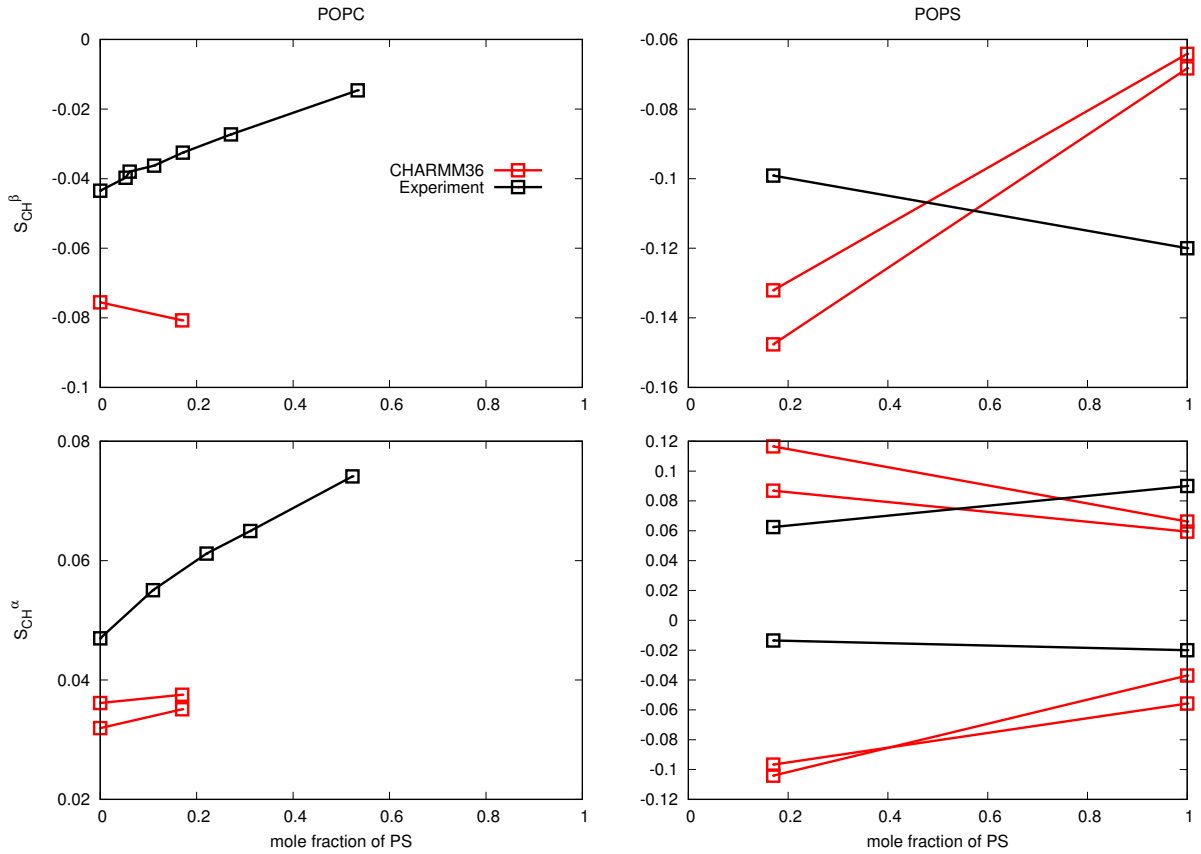

FIG. 7: Headgroup order parameters from PC:PS mixtures from different simulation models and experiments. Left panel shows the PC headgroup order parameters (experimental results from Ref. 4, signs are determined as discussed in [1, 14]). Rigth panel shows PS headgroup order parameters (experimental result for pure POPS measured in this work at 298K, experimental result for mixture from Ref. 15 at 298K). Counterions in expriments are sodium, while potassium is used in simulations. Using sodium in simulations do not have a significant effect.

3.Simulation of CHARMM36 at 298K should be maybe rerun with Gromacs 5.

4.We need results also from other than CHARMM36 force field.

culated from empirical relation $\Delta S_\beta = 0.43\Delta S_\alpha$ [17]. Anyway, the data presented in NMRlipids II project and in Fig. 10 together suggest that Calcium binding is similarly overestimated by CHARMM36 model in pure POPC bilayers and mixtures with POPG. The good agreement of α carbon would be explained by too weak dependence of its order parameter of bound charge

Also dependence of β-carbon of PG on $CaCl_2$ concentration is compared with experiments [10] in Fig. 11. Absolute value of the order parameter is too large without ions, but rapid decrease due to addition of $CaCl_2$ is observed in agreement with experiments for systems with 1:1 mixture of POPC and POPG. In addition, absolute value in systems with $CaCl_2$ is in agreement with experiments. However, system with 4:1 mixture of POPC and POPG behaves differently, but experimental data is not available for comparison for this mixture.

7.More simulation data for systems with negatively charged lipids and $CaCl_2$ to be collected

Effect of Ca2+ binding to PS headgroup

Also the experimental order parameters for PS and PG headgroups as a function of $CaCl_2$ concentration are shown in Fig. 11. **8.These should be compared to simulations for potential structural interpretation of the changes.**

CONCLUSIONS

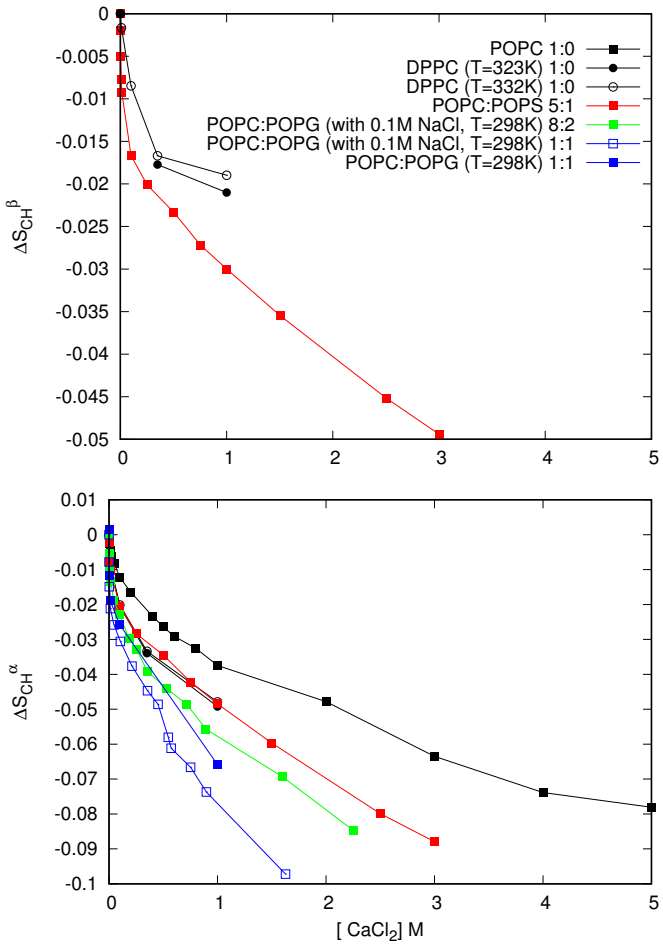

FIG. 8: The change of PC headgroup order parameters in the presence of different amount of negatively charged lipids respect to the values without added $CaCl_2$. The original data is the same as in Fig. **??**.

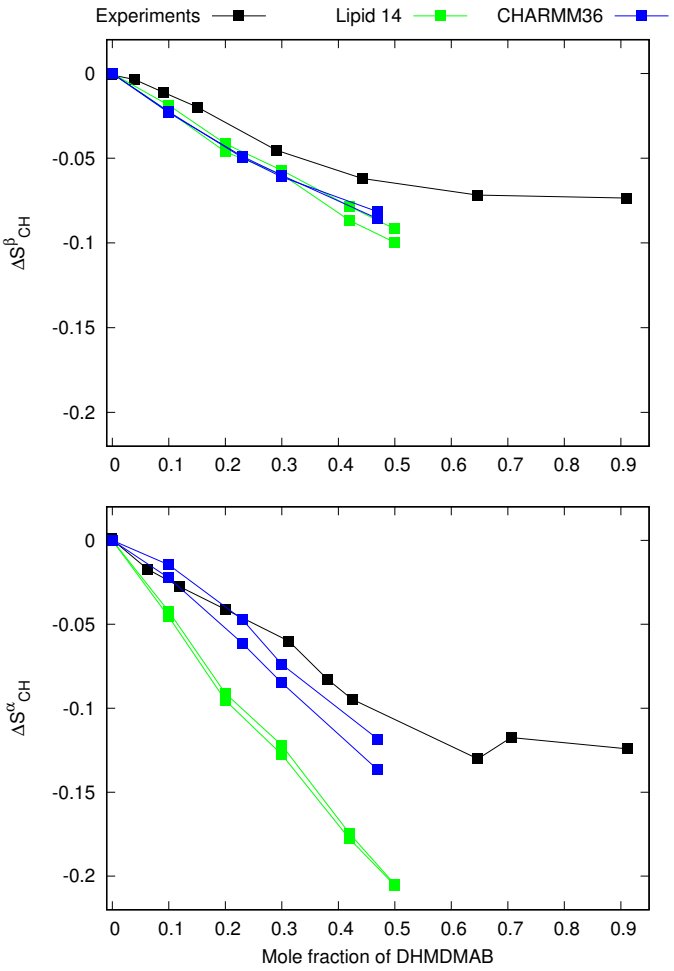

FIG. 9: The response of headgroup order parameters to the fixed amount of cationic surfactants in POPC bilayer is compared between simulations and experiments [13].

SUPPLEMENTARY INFORMATION

Simulated systems

Measurements of order parameter sign

Fig. 12 summarizes the experimental results on the order parameter sign measurement for POPS sample. The experimental protocol is the same used in Ref. 25. In (a) you see the headgroup region of the INEPT spectrum where alpha and beta are identified. In (b) you have the R-PDLF slices for alpha and beta where you see one single splitting for beta (which gives an order parameter equal to 0.12), and for alpha a superposition of a large splitting (order parameter equal to 0.09) and a very small splitting which cannot be calculated. On the bottom you have the S-DROSS slices of these two carbons. The grey lines show a random collection of slices from noise such that it gets clear what is significant. The S-DROSS slice for beta clearly shows that the order parameter is negative. The slice for alpha shows that the higher order parameter is positive and suggests that the smaller order parameter is negative (from the deviation towards negative values in the longer t1 times).

The results updated with SIMPSON simulations for the SDROSS profiles are shown in Fig. 13. The value for the smaller alpha order parameter is taken from Fig 3 in Ref. 26, because resolution in 13C NMR experiments was nor high enough to determine numerical value for this. The plots in Fig. 13 (c) show the following. The error bars and points are the experimental SDROSS data. The thick lines are SIMPSON simulations. The simulations were done by using the order parameter for beta equal to -0.12 and for alpha one order parameter equal to 0.09 and the other equal to -0.02 (black) or 0.02 (grey). Since the black lines agree with experimental data, we conlude that the order parameters for β carbon are -0.12 and for α order parameters are 0.09 and -0.02.

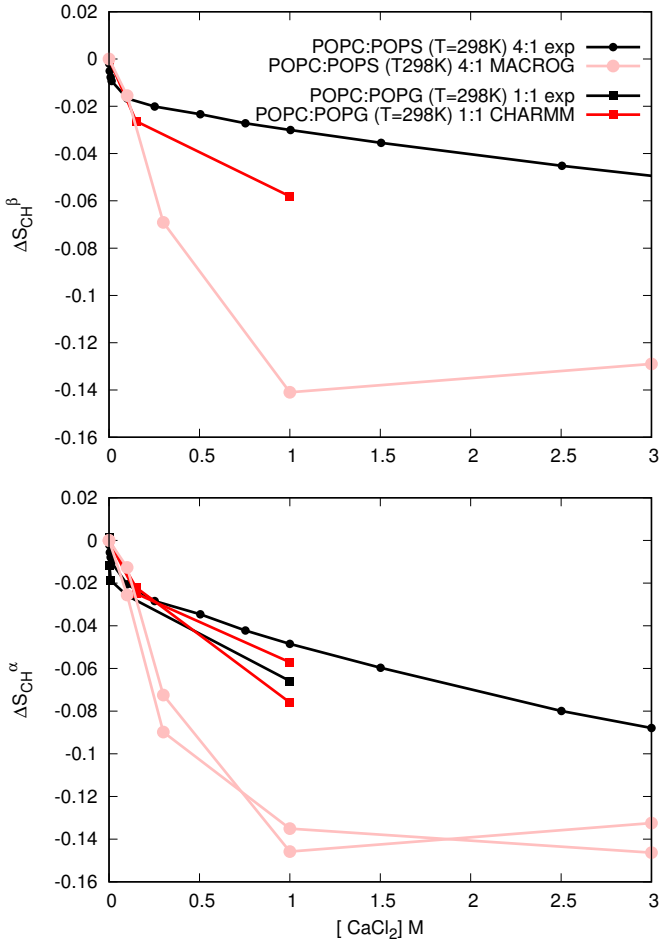

FIG. 10: PG order parameters as a function $CaCl_2$ concentration from experiments [10] and CHARMM36 simulations. Note that beta order parameter is calculated from empirical relation $\Delta S_\beta = 0.43\Delta S_\alpha$ [17], not actually measured.

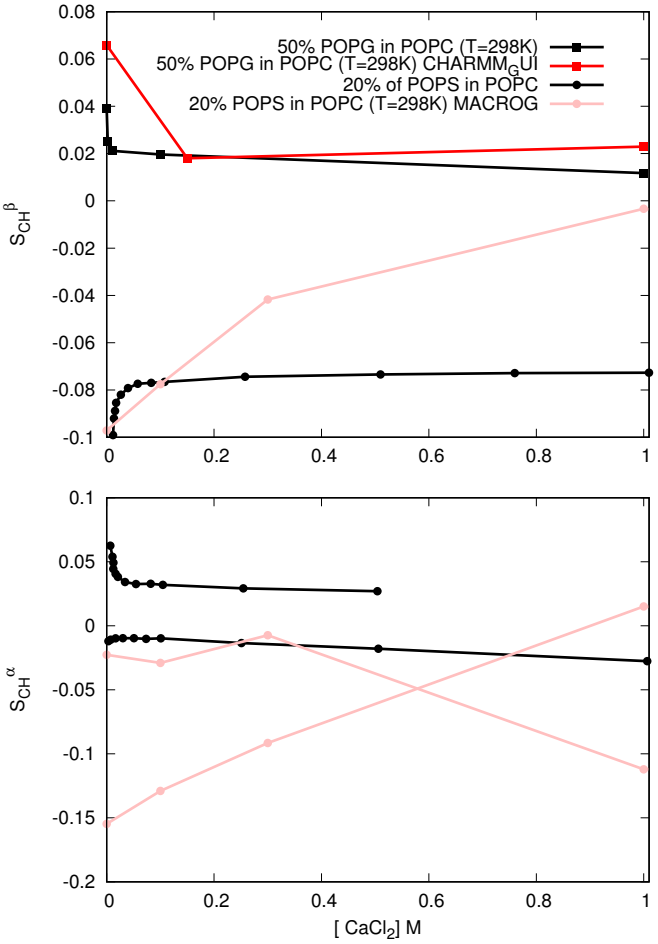

FIG. 11: PG and PS order parameters a function $CaCl_2$ concentration taken from [10] and [15], respectively.

9.Get the small concentration data from the inserts

Details of the rough subjective force field ranking (Fig. 5)

The assessment was based fully on the Fig. 4. First, for each carbon (the columns in Fig. 4) in each force field (the rows), we looked separately at deviations in magnitude and forking.

Magnitude deviations, i.e., how close to the experimentally obtained C–H order parameters (OPs) the force-field-produced OPs were. For each carbon, the following 5-step scale was used:

0 ( ): More than half of all the calculated OPs (that is, of all different hydrogens in all different lipids) were within the *subjective sweet spots* (SSP, blue-shaded areas in Fig. 4).

1 (ᴍ): All the calculated OPs were < 0.03 units away from the SSP.

2 (M): All the calculated OPs were < 0.05 units away from the SSP.

Dihedrals

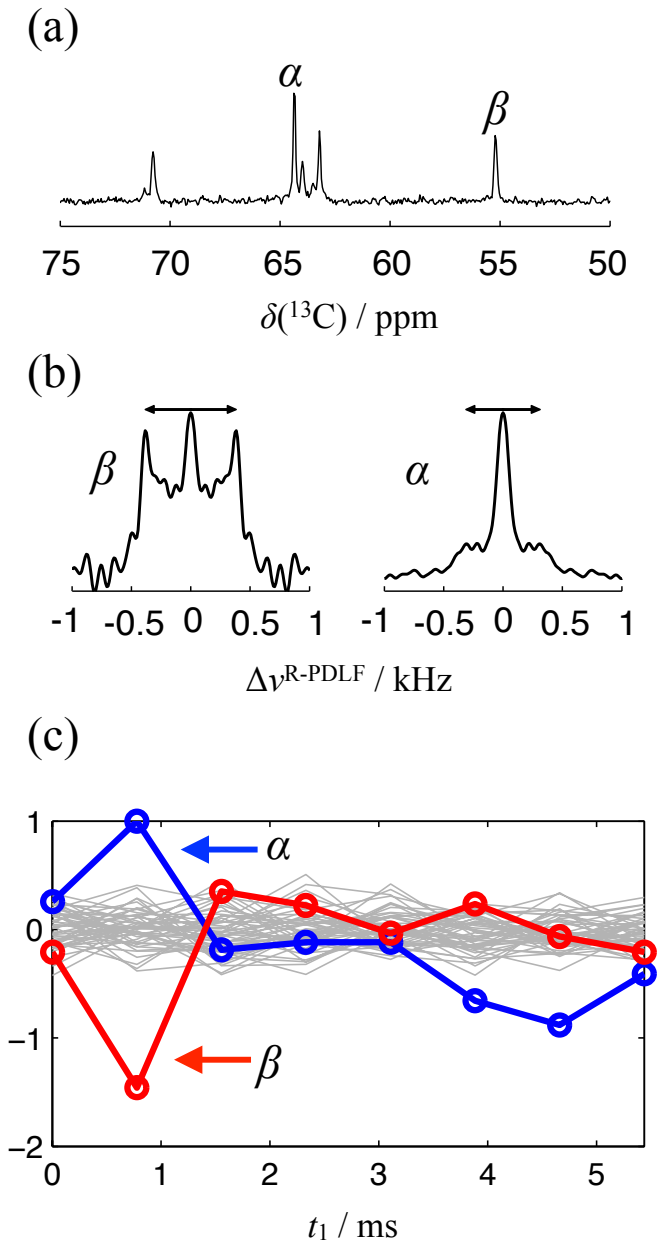

FIG. 12: Experimental results for sign measurement for POPS sample

3 (M): All the calculated OPs were < 0.10 units away from the SSP.

4 (M): Some of the calculated OPs were > 0.10 units away from the SSP.

Forking deviations, i.e., how well the difference in order parameters of two hydrogens attached to a given carbon matched that obtained experimentally. Note that this is not relevant for β and g_2, which have only one hydrogen. For the α carbon, for which a considerable forking of 0.105 is experimentally seen, the following 5-step scale was used:

0 ( ): The distance D between the dots (that mark the measurement-time-weighted averages in Fig. 4) was $0.08 < D < 0.13$ units for all the calculated OPs (that is, for all different lipids).

1 (F): $(0.06 < D < 0.08)$ OR $(0.13 < D < 0.15)$.

2 (F): $(0.04 < D < 0.06)$ OR $(0.15 < D < 0.17)$.

3 (F): $(0.02 < D < 0.04)$ OR $(0.17 < D < 0.19)$.

4 (F): $(D < 0.02)$ OR $(0.19 < D)$.

For the g_3 carbon, for which no forking is indicated by experiments, the following 5-step scale was used:

0 ( ): $D < 0.02$.

1 (F): $0.02 < D < 0.04$.

2 (F): $0.04 < D < 0.06$.

3 (F): $0.06 < D < 0.08$.

4 (F): $0.08 < D$.

For the g_1 carbon, for which a considerable forking of 0.13 is experimentally seen, the following 5-step scale was used:

0 ( ): $0.11 < D < 0.15$.

1 (F): $(0.09 < D < 0.11)$ OR $(0.15 < D < 0.17)$.

2 (F): $(0.07 < D < 0.09)$ OR $(0.17 < D < 0.19)$.

3 (F): $(0.05 < D < 0.07)$ OR $(0.19 < D < 0.21)$.

4 (F): $(D < 0.05)$ OR $(0.21 < D)$.

Based on these assessments of magnitude and forking deviations, each carbon was then assigned to one of the following groups: "within experimental error" (magnitude and forking deviations both on step 0 of the scales described above), "almost within experimental error" (sum of the magnitude and forking deviation steps 1 or 2), "clear deviation from experiments" (sum of magnitude and forking deviation steps from 3 to 5), and "major deviation from experiments" (sum of magnitude and forking deviation steps from 6 to 8). These groups are indicated by colors in Fig. 4. (Note that for β and g_2, for which there can be no forking, the corresponding group assigment limits were: 0, 1, 2, and 3.)

Finally, the total ability of the force field to describe the headgroup and glycerol structure was estimated. To this end, the groups were given the following weights: 0 (within experimental error), 1 (almost within experimental error), 2 (clear deviation from experiments), 4 (major deviation from experiments), and the weights of the five carbons were summed up. The sum, given in the Σ-column of Fig. 4, was then used to (roughly and subjectively, as should be clear from the above description) rank the force fields.

* samuli.ollila@helsinki.fi

[1] A. Botan, F. Favela-Rosales, P. F. J. Fuchs, M. Javanainen, M. Kanduč, W. Kulig, A. Lamberg, C. Loison, A. Lyubartsev, M. S. Miettinen, et al., J. Phys. Chem. B **119**, 15075 (2015).

[2] A. Catte, M. Girych, M. Javanainen, C. Loison, J. Melcr, M. S. Miettinen, L. Monticelli, J. Maatta, V. S. Oganesyan, O. H. S. Ollila, et al., Phys. Chem. Chem. Phys. **18**, 32560 (2016).

[3] H. U. Gally, G. Pluschke, P. Overath, and J. Seelig, Biochemistry **20**, 1826 (1981).

[4] P. Scherer and J. Seelig, EMBO J. **6** (1987).

[5] J. Seelig, Cell Biology International Reports **14**, 353 (1990), ISSN 0309-1651, URL http://www.sciencedirect.com/science/article/pii/030916519091204H.

[6] R. Wohlgemuth, N. Waespe-Sarcevic, and J. Seelig, Biochemistry **19**, 3315 (1980).

[7] G. Büldt and R. Wohlgemuth, The Journal of Membrane Biology **58**, 81 (1981), ISSN 1432-1424, URL http://dx.doi.org/10.1007/BF01870972.

[8] T. M. Ferreira, F. Coreta-Gomes, O. H. S. Ollila, M. J. Moreno, W. L. C. Vaz, and D. Topgaard, Phys. Chem. Chem. Phys. **15**, 1976 (2013).

[9] J. L. Browning and J. Seelig, Biochemistry **19**, 1262 (1980).

[10] F. Borle and J. Seelig, Chemistry and Physics of Lipids **36**, 263 (1985).

[11] J. Seelig and H. U. Gally, Biochemistry **15**, 5199 (1976).

[12] J. Seelig, P. M. MacDonald, and P. G. Scherer, Biochemistry **26**, 7535 (1987).

[13] P. G. Scherer and J. Seelig, Biochemistry **28**, 7720 (1989).

[14] O. S. Ollila and G. Pabst, Biochimica et Biophysica Acta (BBA) - Biomembranes **1858**, 2512 (2016).

[15] M. Roux and M. Bloom, Biochemistry **29**, 7077 (1990).

[16] P. M. Macdonald and J. Seelig, Biochemistry **26**, 1231 (1987).

[17] H. Akutsu and J. Seelig, Biochemistry **20**, 7366 (1981).

[18] J. P. M. Jämbeck and A. P. Lyubartsev, J. Chem. Theory Comput. **8**, 2938 (2012).

[19] F. Favela-Rosales, *MD simulation trajectory of a fully hydrated DPPE bilayer: SLIPIDS, Gromacs 5.0.4. 2017.* (2017), URL https://doi.org/10.5281/zenodo.495247.

[20] J. P. M. Jämbeck and A. P. Lyubartsev, Phys. Chem. Chem. Phys. **15**, 4677 (2013).

[21] F. Favela-Rosales, *MD simulation trajectory of a fully hydrated DOPS bilayer: SLIPIDS, Gromacs 5.0.4. 2017.* (2017), URL https://doi.org/10.5281/zenodo.495510.

[22] P. Mukhopadhyay, L. Monticelli, and D. P. Tieleman, Biophysical Journal **86**, 1601 (2004).

[23] J. B. Klauda, R. M. Venable, J. A. Freites, J. W. O'Connor, D. J. Tobias, C. Mondragon-Ramirez, I. Vorobyov, A. D. MacKerell Jr, and R. W. Pastor, J. Phys. Chem. B **114**, 7830 (2010).

[24] O. H. S. Ollila, *POPS+83%popc lipid bilayer simulation at T298K ran CHARMM_GUI force field and Gromacs* (2017), URL https://doi.org/10.5281/zenodo.1011104.

[25] T. M. Ferreira, R. Sood, R. Bärenwald, G. Carlström, D. Topgaard, K. Saalwächter, P. K. J. Kinnunen, and O. H. S. Ollila, Langmuir **32**, 6524 (2016).

[26] M. Roux and M. Bloom, Biophys. J. **60**, 38 (1991).

ToDo

TABLE I: List of MD simulations. The salt concentrations calculated as [salt]=$N_c \times$[water] / N_w, where [water] = 55.5 M.

lipid/counter-ions	force field for lipids / ions	NaCl (mM)	$CaCl_2$ (mM)	[a]N_l	[b]N_w	[c]N_c	[d]T (K)	[e]t_{sim}(ns)	[f]t_{anal} (ns)	[g]files
DPPE	Slipids [18]	0	0	288	9386	0	336	200	100	[19]
DOPS/Na^+	CHARMM36 [?] 10.	0	0	128	4480	0	303	500	100	[?] 11.
DOPS/Na^+	CHARMM36ua [?] 12.	0	0	128	4480	0	303	500	100	[?] 13.
DOPS/Na^+	Slipids [20]	0	0	128	4480	0	303	500	100	[?] 14.
DOPS/Na^+	Slipids [20]	0	0	288	11232	0	303	200	100	[21]
DOPS/Na^+	Berger [22]	0	0	128	4480	0	303	500	100	[?] 15.
DOPS/Na^+	GROMOS-CKP [?] 16.	0	0	128	4480	0	303	500	100	[?] 17.
POPS/Na^+	CHARMM36 [?] 18.	0	0	128	4480	0	298	500	100	[?] 19.
POPS/Na^+	CHARMM36ua [?] 20.	0	0	128	4480	0	298	500	100	[?] 21.
POPS/Na^+	Slipids [20]	0	0	128	4480	0	298	500	100	[?] 22.
POPC:POPS (5:1)/K^+	CHARMM36 [23?] 23.	0	0	110:22	4935	0	298	100	100 24.	[24]

[a]Number of lipid molecules with largest mole fraction
[b]Number of water molecules
[c]Number of additional cations
[d]Simulation temperature
[e]Total simulation time
[f]Time used for analysis
[g]Reference for simulation files

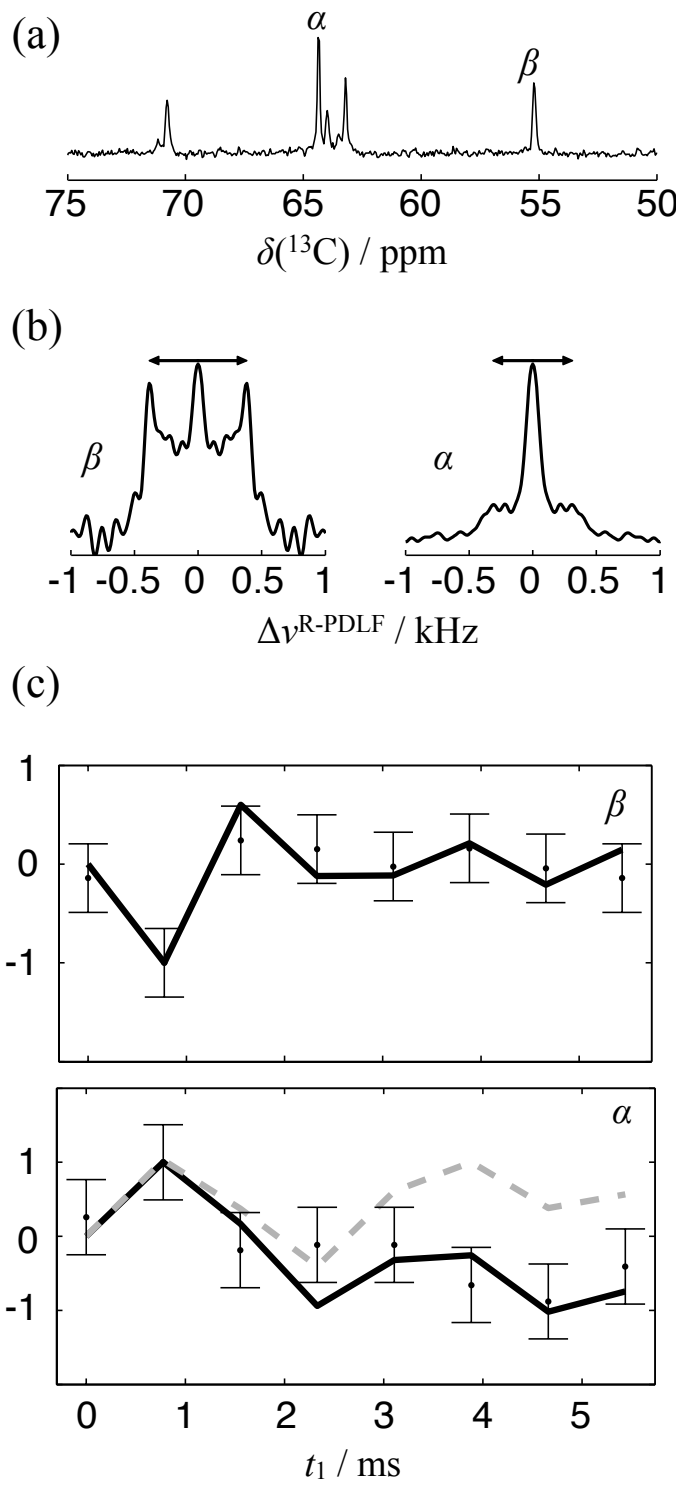

FIG. 13: Experimental results for sign measurement for POPS sample

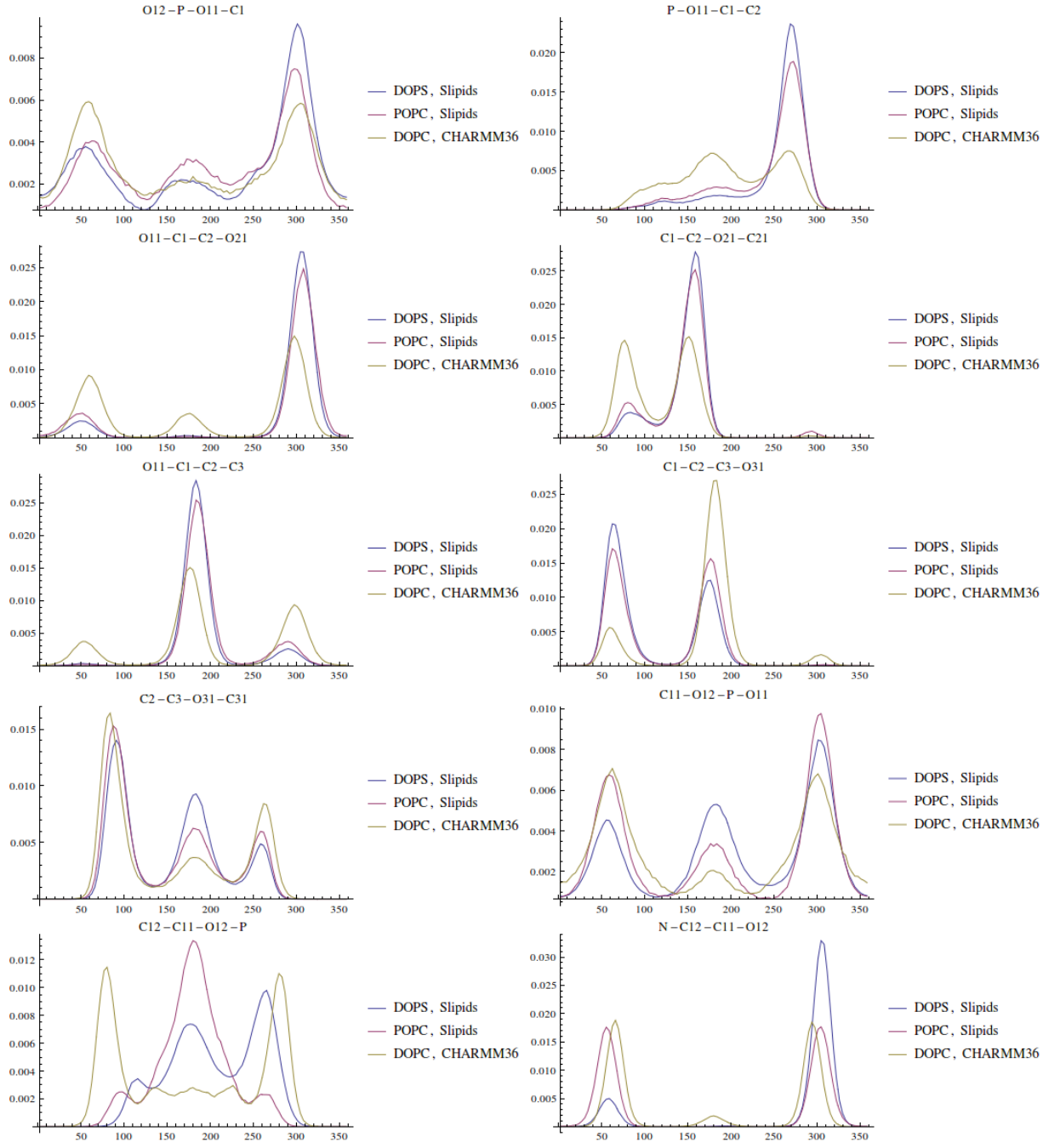

FIG. 14: Experimental results for sign measurement for POPS sample